ISSN 0023-1584, Kinetics and Catalysis, 2006, Vol. 47, No. 1, pp. 106–120. © MAIK "Nauka/Interperiodica" (Russia), 2006.
Original Russian Text © T.I. Drozdova, E.T. Denisov, A.F. Shestakov, N.S. Emel'yanova, 2006, published in Kinetika i Kataliz, 2006, Vol. 47, No. 1, pp. 111–123.

Geometry of the Transition State of Radical Abstraction Reactions Involving Si–H, Ge–H, and Sn–H Bonds

T. I. Drozdova, E. T. Denisov, A. F. Shestakov, and N. S. Emel'yanova

Institute of Chemical Physics in Chernogolovka, Russian Academy of Sciences, Chernogolovka, Moscow oblast, 142432 Russia

Received April 22, 2004

Abstract—Transition-state interatomic distances in the reactions $C^{\bullet}H_3 + SiH_4$, $Si^{\bullet}H_3 + SiH_4$, $C^{\bullet}H_3 + GeH_4$, and $C^{\bullet}H_3 + SnH_4$ are calculated by the B3LYP density functional and intersecting parabolas methods. A semiempirical algorithm is developed for the calculation of the Y…H and C…H distances in the transition state of the radical abstraction reactions $R^{\bullet} + YH$ involving silanes, germanes, and stannanes and the reverse reactions of silyl, germanyl, and stannyl radicals with hydrocarbons. This algorithm is used to calculate interatomic distances in these reactions. An analysis of the calculated data shows that the Y…H and C…H distances in these reactions depend on the following factors: the enthalpy of reaction, the radius of the Y atom (Y = C, Si, Ge, Sn), and four-electron repulsion during the attack of a radical on the C–H bond adjacent to the double bond. Empirical equations relating the interatomic distances to the enthalpy of reaction and to the Y–R bond length are set up.

DOI: 10.1134/S0023158406010162

Previously, we examined radical abstraction reactions involving silanes, germanes, and stannanes in the framework of the intersecting parabolas model (IPM) [1]. This analysis showed that the activation energy of these reactions depends on several factors, including the radius of the atom in the reaction center of the transition state (TS): the longer the radius of the Y atom in the reaction center R…H…Y of the abstraction reaction, the higher the activation energy.

The present work deals with the geometry of the TS in these reactions. The interatomic distances for the reactions of alkyl radicals with R_3SiH, R_3GeH, and R_3SnH were calculated from experimental data using the IPM. For comparison, we performed a quantum-chemical calculation of the TS geometry for the reactions of methyl radicals with SiH_4, GeH_4, and SnH_4. A comparison of the TS interatomic distances obtained by the density functional theory (DFT) and IPM calculations made it possible to develop a semiempirical method for calculating TS interatomic distances for the reactions considered. Here we use this method to calculate the TS interatomic distances and analyze the factors in the TS geometry.

COMPUTATIONAL PROCEDURE

DFT Calculation

The B3LYP hybrid density functional was used in the theoretical study of radical abstraction reactions of the type

$$C^{\bullet}H_3 + H–YH_3 \longrightarrow CH_3–H + Y^{\bullet}H_3,$$

where Y = Si, Ge, and Sn, and of the symmetrical reaction

$$Si^{\bullet}H_3 + SiH_4 \longrightarrow SiH_4 + Si^{\bullet}H_3.$$

Calculations were carried out using the Gaussian 98 program [2]. The geometry of stationary points was optimized in the 6-31G* basis set. The optimized geometry was used in the calculation of the energy of the system in the 6-311++G(d,p) basis set taking into account the zero-point energies in the B3LYP/6-31G* approximation. A comparison between the geometry of the $CH_3C…H…SiH_3$ TS obtained with the 6-311++G** extended basis set [3] and the geometry determined in this work reveals small differences not exceeding 0.005 Å in the interatomic distances. In the case of the Sn-containing system, the LANL2DZ basis set was used in the optimization of the geometry and in the calculation of the energy of the system. As is demonstrated by the comparative analysis for the Ge-containing system, the TS structures obtained in the LANL2DZ and 6-31G* basis sets differ insignificantly. The data calculated for the above abstraction reactions are given in Table 1. The TS structures are presented in Fig. 1 along with the frequencies of the imaginary vibrations in the TS.

As is shown in Fig. 1, the TS's in the reactions are characterized by linear geometries of the reaction centers Si…H…Si and C…H…Y. Since the reactions involving the methyl radical are exothermic, their TS's can be regarded as early. Correspondingly, the C…Y distance elongates with an increase in the radius of the Y atom: $r^{\#}(C…Y) = 3.23 \times 10^{-10}$ m for Y = Si, 3.37 ×

Table 1. Total energy (E), zero-point energy (ZPE), and the geometric parameters of the reactants and transition states calculated by the B3LYP method

System and its symmetry	Geometric parameters		E(B3LYP/6-31G*), at. units	Hartree ZPE	E(B3LYP/6-311++G**), at. units	ΔH, E,* kJ/mol
	bond length $\times 10^{10}$, m	angle, deg				
			$Si^{\bullet}H_3 + SiH_4 \longrightarrow SiH_4 + Si^{\bullet}H_3$			
$Si^{\bullet}H_3$, C_{3v}	1.489 (Si–H)	110.9 (H–Si–H)	–291.23226	0.02128	–291.26130	$\Delta H = 0$
SiH_4, T_d	1.486 (Si–H)	–	–291.88369	0.03132	–291.91427	E = 26.3(46.8)
$SiH_3H^*SiH_3$ (TS), C_{3v}	1.775 (Si–H*)	109.1 (H*–Si–H)	–583.10266	0.04966	–583.16262	[28.5]
			$C^{\bullet}H_3 + SiH_4 \longrightarrow CH_4 + Si^{\bullet}H_3$			
$C^{\bullet}H_3$, D_{3h}	1.083 (C–H)	–	–39.83829	0.02981	–39.85517	ΔH = –53.6
CH_4, T_d	1.093 (C–H)	–	–40.51839	0.04522	–40.53394	(–55.9)
$CH_3H^*SiH_3$	1.616 (C–H*),	101.6 (H*–C–H),	–331.71278	0.06193	–331.758783	E = 30.1(29.4)
(TS), C_{3v}	1.614 (Si–H*)	110.0 (H*–Si–H)	–	–	–	[31.1]
			$C^{\bullet}H_3 + GeH_4 \longrightarrow CH_4 + Ge^{\bullet}H_3$			
GeH_4, T_d	1.539 (Ge–H)	–	–2077.36111	0.02900	–2079.40441	ΔH = –77.9
$Ge^{\bullet}H_3$, C_{3v}	1.548 (Ge–H)	110.4 (H–Ge–H)	–2076.71983	0.01955	–2078.76127	[–67.9]
$CH_3H^*GeH_3$	1.734 (C–H*),	99.5 (H*–C–H),	–2117.19795	0.06054	–2119.25293	E = 22.0
(TS), C_{3v}	1.615 (Ge–H*)	110.2 (H*–Ge–H)	–	–	–	[26.6]
			B3LYP/LANL2DZ			
			$C^{\bullet}H_3 + GeH_4 \longrightarrow CH_4 + Ge^{\bullet}H_3$			
GeH_4, T_d	1.544 (Ge–H)	–	–6.14714	0.02915	–	ΔH = –82.5
$Ge^{\bullet}H_3$, C_{3v}	1.552 (Ge–H)	110.3 (H–Ge–H)	–5.50828	0.01968	–	E = 18.7
$CH_3H^*GeH_3$	1.734 (C–H*),	98.9 (H*–C–H),	–	–	–	
(TS), C_{3v}	1.637 (Ge–H*)	110.0 (H*–Ge–H)	–45.97836	0.06011	–	
			$C^{\bullet}H_3 + SnH_4 \longrightarrow CH_4 + Sn^{\bullet}H_3$			
$C^{\bullet}H_3$, D_{3h}	1.086 (C–H)	–	–39.83738	0.02998	–	ΔH = –115.8
CH_4, T_d	1.095 (C–H)	–	–40.51447	0.04524	–	[–71.3]
SnH_4, T_d	1.712 (Sn–H)	–	–5.73634	0.02570	–	E = 14.4
$Sn^{\bullet}H_3$, C_{3v}	1.724 (Sn–H)	108.9 (H–Sn–H)	–5.11032	0.01740	–	[27.1]
$CH_3H^*SnH_3$	1.884 (C–H*),	97.0 (H*–C–H)	–45.56964	0.05708	–	
(TS), C_{3v}	1.780 (Sn–H*)	110.3 (H*–Sn–H)	–	–	–	

* The experimental values of ΔH_e and E for the reactions $CH_3^{\bullet} + SiH_4$ [4] and $Si^{\bullet}H_3 + SiH_4$ [5] are given in parentheses, and the same parameters from Table 3 calculated by the IPM using formulas (2), (4), and (5) on the basis of ΔH_e and $E_{e,0}$ from Table 2 are given in brackets.

10^{-10} m for Y = Ge, and 3.66×10^{-10} m for Y = Sn. These distances are close to the distances obtained by MP2/DZP nonempirical calculations [6, 7]—3.15×10^{-10}, 3.26×10^{-10}, and 3.50×10^{-10} m, respectively—and to the results of MP2 calculations in the 6-31G* basis set ($r^{\#}$(C…Si) = 3.17×10^{-10} m) and in the LANL2DZ/31G* basis set $r^{\#}$(C…Ge) = 3.28×10^{-10} m and $r^{\#}$(C…Sn) = 3.53×10^{-10} m) [8]. Shorter $r^{\#}$(C…Y) distances are obtained for the semiempirical model of intersecting states [9] ($r^{\#}$(C…Si) = 3.07×10^{-10} m and

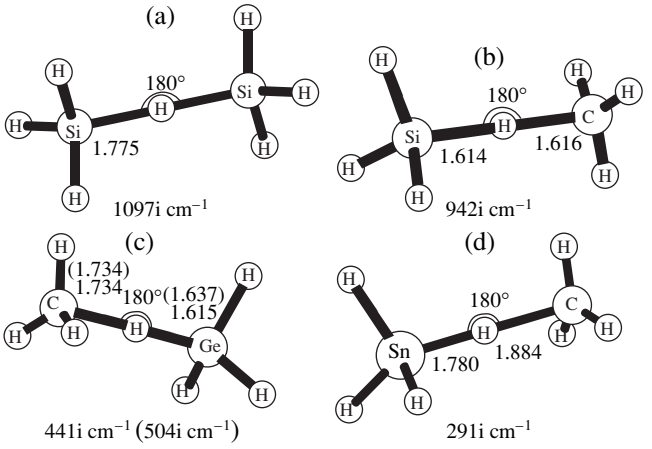

Fig. 1. Transition state structures in the reactions (a) $H_3Si^{\cdot}$ + H–SiH_3 ⟶ H–SiH_3 + $H_3Si^{\cdot}$ and (b–d) $C^{\cdot}H_3$ + H–YH_3 ⟶ CH_3–H + $Y^{\cdot}H_3$, where Y = (b) Si, (c) Ge, and (d) Sn. The distances are expressed in m ($\times 10^{10}$), and the results of the B3LYP/LANL2DZ calculation are presented in parentheses. The frequencies of imaginary vibrations of the H atom in the TS are given under each structure. The distances are in 10^{-10} m.

$r^{\#}$(C…Ge) = 3.15×10^{-10} m), except for $r^{\#}$(Si…Si) = 3.54×10^{-10} m, which is close to our value of 3.55×10^{-10} m. This model gives the activation energy (E) values differing by at most 4 kJ/mol from the values found experimentally or values calculated using the IPM. However, the elongation of the H–Y bond in the TS becomes negative (bond contraction), and, hence, the TS structure predicted by this method is unreliable. The MP2 $r^{\#}$(C…Y) distances are shorter than the B3LYP distances primarily because of a shorter $r^{\#}$(C…H) distance. The difference between the MP2 and B2LYP values of the latter increases from 0.09×10^{-10} to 0.18×10^{-10} m on passing from Y = Si to Y = Sn.

Thus, the MP2 method predicts a later TS for the reactions of the methyl radicals with YH_4. This implies appreciably higher energy (E) values in the MP2 approach (E = 53–54 kJ/mol (SiH_4), 35–42 kJ/mol (GeH_4), and 34–35 kJ/mol (SnH_4)) as compared to experimental data or IPM estimates [6–8]. Use of the QCISD approach in the calculation of the energy from the MP2/DZP TS geometry does not change the situation, because this approach decreases the activation energy by no more than 2 kJ/mol [6, 7]. For the reaction $Si^{\cdot}H_3 + SiH_4$, the QCISD approach using the geometry calculated by the MP2/6-31G* method leads to an overestimated E value of 65.7 kJ/mol [10]. In view of this discrepancy, we believe that the B3LYP TS geometry is less erroneous. The discrepancy will be particularly significant if we take into account that, with overestimated activation energies, the MP2 method gives, as a rule, an overestimated heat of reaction. For Y = Sn, the overestimation is 33 kJ/mol for the DZP basis set [9] and 57 kJ/mol for the LANL2DZ/31G* basis set [8].

Calculation Using the Intersecting Parabolas Method

Radical abstraction reactions of the type

$$X^{\cdot} + HYH_3 \longrightarrow XH + Y^{\cdot}H_3$$

in the framework of the IPM are characterized by the following parameters [11–14]:

(1) the enthalpy ΔH_e that includes the difference between the zero-point energies of the breaking and forming bonds,

$$\Delta H_e = D(\text{H–Y}) - D(\text{X–H}) + 0.5hN_A(\nu(\text{H–Y}) - \nu(\text{X–H})), \quad (1)$$

where ν(H–Y) and ν(X–H) are the vibration frequencies of the breaking and forming bonds, respectively;

(2) the classical potential barrier E_e, which includes the zero-point energy of the breaking bond and is correlated with the Arrhenius (experimental) activation energy as

$$E_e = E + 0.5(hN_A\nu(\text{H–Y}) - RT); \quad (2)$$

(3) the parameter r_e, which is equal to the total extension of the breaking H–Y and forming X–H bonds in the TS;

(4) the parameter b ($2b^2$ is the force constant of the breaking H–Y bond);

(5) the parameter α (α^2 is the ratio of the force constants of the breaking and forming bonds); and

(6) the preexponential factor A_0 per equireactive bond in the molecule.

The reaction rate constant is related to E and A_0 by the Arrhenius formula

$$k = nA_0\exp(-E/RT), \quad (3)$$

Table 2. Parameters of radical abstraction reactions for the IPM

R_3Y–H bond	r(H–Y) $\times 10^{10}$, m	$b \times 10^{10}$, (kJ/mol)$^{1/2}$ m^{-1}	$0.5hN_A\nu$(H–Y), kJ/mol
R_3C–H	1.092 (1.093 in CH_4)	37.43	17.4
R_3Si–H	1.483 (1.480 in SiH_4)	28.71	13.1
R_3Ge–H	1.525	27.95	12.6
R_3Sn–H	1.711	26.97	12.1

Table 3. Kinetic parameters of radical abstraction reactions for the IPM [1, 11]

Class of reactions*	α	$E_{e,0}$, kJ/mol	br_e, (kJ/mol)$^{1/2}$	$A_0 \times 10^{-9}$, l mol^{-1} s^{-1}	$r_e \times 10^{10}$, m	$0.5hN_A(\nu(Y–H) – \nu(X–H))$, kJ/mol
$R^{1\bullet} + R^1–H$	1.000	74.7	17.29	1.0	0.462	0
$R^{1\bullet} + R_3Si–H$	0.767	55.6	13.18	1.0	0.459	–4.3
$R^{1\bullet} + R_3Ge–H$	0.747	62.6	13.82	1.0	0.494	–4.8
$R^{1\bullet} + R_3Sn–H$	0.721	63.1	13.67	1.0	0.507	–5.3
$R_3Si^\bullet + R^1–H$	1.304	55.6	17.18	2.0	0.459	4.3
$R_3Si^\bullet + R^2–H$	1.304	63.8	18.40	0.1	0.492	4.3
$R_3Si^\bullet + R^3–H$	1.304	58.7	17.65	0.1	0.472	4.3
$R_3Si^\bullet + R_3Si–H$	1.000	46.8	13.69	2.0	0.477	0
$R_3Ge^\bullet + R^1–H$	1.339	62.6	18.50	2.0	0.494	4.8
$R_3Sn^\bullet + R^1–H$	1.387	63.1	18.96	2.5	0.507	5.3

* R, R^1, R^2, and R^3 are the radicals of organic compounds of different classes (see below).

where n is the number of equireactive bonds in the reactant molecule. The coefficients b, the zero-point energies of the bonds [1, 11], and the equilibrium distances between the Y and H atoms in the molecules of the classes of compounds considered [15] are given in Table 2.

The above-listed parameters in the IPM are related by the equation [11]

$$br_e = \alpha\sqrt{E_e - \Delta H_e} + \sqrt{E_e}. \quad (4)$$

An analysis of experimental data shows that the parameters α, b, A_0, and r_e characterize the whole class of reactions and are almost the same for all individual reactions of this class [11–14]. Their values are given in Table 3.

The constancy of r_e inside a reaction class is confirmed by the results of nonempirical calculations [6, 7], which show that the introduction of alkyl radicals at the C (in $X^\bullet$) or Y (in HY) atom changes the $r^{\#}$(C…Y) distance by at most 0.02×10^{-10} m, while the changes in $r^{\#}$(C…H) and $r^{\#}$(H…Y) are as large as 0.05×10^{-10} and 0.12×10^{-10} m, respectively. Knowing the br_e parameter, one can calculate the classical potential barrier E_e from the enthalpy of the reaction,

$$\sqrt{E_e} = br_e \frac{1 + \dfrac{\alpha\Delta H_e}{(br_e)^2}}{1 + \alpha\sqrt{1 - \dfrac{1-\alpha^2}{(br_e)^2}\Delta H_e}}, \quad (5)$$

and calculate the classical potential barrier $E_{e,0}$ for a thermally neutral reaction (for which $\Delta H_e = 0$),

$$E_{e,0} = \frac{(br_e)^2}{(1+\alpha)^2}. \quad (6)$$

The position of the hydrogen atom being abstracted in the TS (H…Y) in the r_e interval is characterized by an $r^{\#}$ distance, which, in the IPM, is calculated by the formula [11]

$$r^{\#} = \frac{r_e\sqrt{E_e}}{\alpha\sqrt{E_e - \Delta H_e} + \sqrt{E_e}}. \quad (7)$$

The X…H distance in the TS is determined as

$$r_e - r^{\#} = \frac{\alpha r_e\sqrt{E_e - \Delta H_e}}{\alpha\sqrt{E_e - \Delta H_e} + \sqrt{E_e}}. \quad (8)$$

Semiempirical Method for Calculating TS Interatomic Distances

DFT calculations give larger bond extension values in the TS than does the IPM (Table 4). The coefficient β is the ratio of the total extensions of the reacting

Table 4. Total extensions of the X...H...Y bonds in the TS calculated by the DFT and IPM methods and their ratio (β)

Reaction	$r_e \times 10^{10}$, m (IPM)	$\Delta r^{\#}$(X...H...Y) $\times 10^{10}$, m (DFT)	β
$C^\bullet H_3 + SiH_4$	0.459	0.655	1.427
$Si^\bullet H_3 + SiH_4$	0.477	0.584	1.224
$C^\bullet H_3 + GeH_4$	0.494	0.753	1.524
$C^\bullet H_3 + SnH_4$	0.507	0.861	1.698

Table 5. Enthalpy, activation energy, rate constant, and TS geometry calculated by formulas (1)–(5), (9), and (10) for hydrogen atom abstraction from silanes, germanes, and stannanes by the $(CH_3)_2C^{\bullet}H$ radical

Compound Y–H	D(Y–H), kJ/mol	ΔH_e, kJ/mol	E, kJ/mol	k (350 K), l mol^{-1} s^{-1}	$r^{\#}$(Y...H) × 10^{10}, m	$r^{\#}$(C...H) × 10^{10}, m
$(CH_3)_2C^{\bullet}H + R_3Si–H$						
$(Me_3Si)_3Si–H$	351.0	–65.3	20.0	1.0×10^6	1.763	1.467
$Ph_3Si–H$	354.8	–61.5	21.2	6.9×10^5	1.768	1.462
$Ph_2MeSi–H$	359.2	–57.1	22.6	4.3×10^5	1.774	1.456
$(Me_3C)_3Si–H$	362.3	–54.0	23.6	3.0×10^5	1.778	1.452
$PhMe_2Si–H$	364.0	–52.3	24.1	2.5×10^5	1.780	1.450
$(MeS)_3Si–H$	366.0	–50.3	24.8	2.0×10^5	1.783	1.447
PhMeClSi–H	369.6	–46.7	26.0	1.3×10^5	1.788	1.442
$(Me_3C)_2MeSi–H$	372.8	–43.5	27.1	9.1×10^4	1.792	1.438
$(Me_3Si)Me_2Si–H$	378.0	–38.3	28.9	4.8×10^4	1.800	1.430
$Cl_3Si–H$	382.0	–34.3	30.3	3.0×10^4	1.805	1.425
$H_3Si–H$	384.1	–32.2	31.1	9.1×10^4	1.808	1.422
$MeH_2Si–H$	386.0	–30.3	31.8	5.4×10^4	1.811	1.419
$Me_2HSi–H$	391.7	–24.6	34.0	1.7×10^4	1.819	1.411
$Et_3Si–H$	398.0	–18.3	36.4	3.7×10^3	1.827	1.402
$F_3Si–H$	419.0	2.7	45.2	1.8×10^2	1.858	1.372
$(CH_3)_2C^{\bullet}H + R_3Ge–H$						
$(Me_3Si)_3Ge–H$	305.2	–111.6	14.5	6.8×10^6	1.801	1.569
$Ph_3Ge–H$	322.5	–94.3	19.0	1.5×10^6	1.824	1.546
$(PhCH_2)_3Ge–H$	324.9	–91.9	19.6	1.2×10^6	1.827	1.543
$(PhCH_2)EtHGe–H$	341.6	–75.2	24.4	4.6×10^5	1.850	1.520
$Bu_3Ge–H$	347.3	–69.5	26.1	1.3×10^5	1.857	1.512
$H_3Ge–H$	348.9	–67.9	26.6	4.3×10^5	1.860	1.510
$(CH_3)_2C^{\bullet}H + R_3Sn–H$						
$Ph_3Sn–H$	296.9	–120.4	14.2	7.7×10^6	2.025	1.639
$Me_3Sn–H$	318.5	–98.8	19.4	1.3×10^6	2.056	1.608
$H_3Sn–H$	346.0	–71.3	27.1	3.7×10^5	2.098	1.566

bonds in the TS calculated using DFT and IPM (parameter r_e). Using r_e, the TS interatomic distances for the reaction classes considered can be refined by the following modified IPM formulas:

$$r^{\#}(\mathrm{H}\ldots\mathrm{Y}) = r(\mathrm{H–Y}) + \beta b^{-1}\sqrt{E_e}, \quad (9)$$

$$r^{\#}(\mathrm{X}\ldots\mathrm{H}) = r(\mathrm{X–H}) + \alpha\beta b^{-1}\sqrt{E_e - \Delta H_e}. \quad (10)$$

The TS interatomic distance X…H…Y is a sum consisting of four terms:

$$r^{\#}(\mathrm{X}\ldots\mathrm{H}\ldots\mathrm{Y}) = r(\mathrm{H–Y}) + r(\mathrm{X–H}) + \beta b^{-1}\sqrt{E_e} + \alpha\beta b^{-1}\sqrt{E_e - \Delta H_e}. \quad (11)$$

RESULTS AND DISCUSSION

Effect of the Enthalpy of Reaction

The results of the calculation of the activation energy and TS interatomic distances by formulas (5),

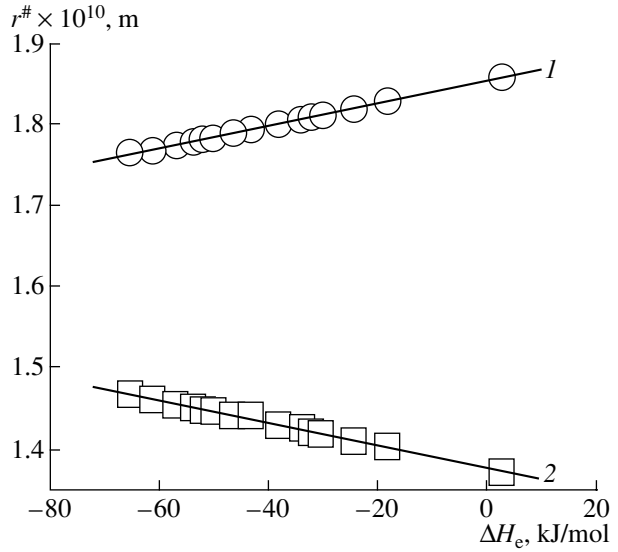

Fig. 2. (*1*) $r^{\#}$(H…Si) and (*2*) $r^{\#}$(C…H) interatomic distances in the TS versus the enthalpy ΔH_e of the reaction $Me_2C^{\bullet} + R_3Si{-}H \longrightarrow Me_2C{-}H + R_3Si^{\bullet}$.

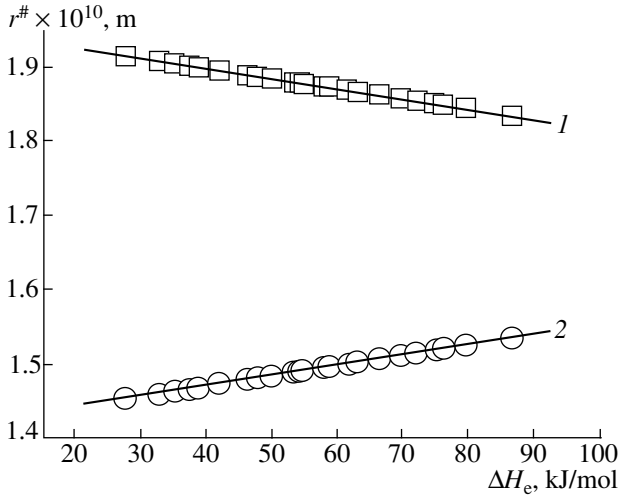

Fig. 3. (*1*) $r^{\#}$(H…Ge) and (*2*) $r^{\#}$(H…C) interatomic distances in the TS versus the enthalpy ΔH_e of the reaction $Bu_3Ge^{\bullet} + R{-}H \longrightarrow Bu_3Ge{-}H + R^{\bullet}$.

(9), and (10) for the reactions of the methylethyl radical with a series of silanes, germanes, and stannanes are listed in Table 5. The data presented in Table 3, the β values found, and the bond dissociation energies D(H–Y) and D(X–H) from [14] were used in this calculation.

The calculated data show that the $r^{\#}$(H…Y) distance elongates with an increase in the enthalpy of reaction (ΔH_e), while $r^{\#}$(C…H) shortens. The plots of $r^{\#}$(H…Y) and $r^{\#}$(C…H) versus ΔH_e are virtually linear (Fig. 2).

A linear relationship of the type $r^{\#} = F + G\Delta H_e$ also follows from formulas (9) and (10). Indeed, at low ΔH_e values (ΔH_e ($|\Delta H_e| \ll (br_e)^2/(1 - \alpha^2)$), formula (5), in view of Eq. (6), takes the form

$$\sqrt{E_e} \approx \frac{br_e}{1+\alpha} + \frac{\alpha\Delta H_e}{2br_e} = \sqrt{E_{e,0}} + \frac{\alpha\Delta H_e}{2(1+\alpha)\sqrt{E_{e,0}}}. \quad (12)$$

Substituting Eq. (12) into Eqs. (9) and (10), we obtain the following equations relating the TS interatomic distances to the enthalpies:

$$r^{\#}(\text{Y}\ldots\text{H}) \approx r(\text{Y–H}) + \frac{\beta\sqrt{E_{e,0}}}{b}\left(1 + \frac{\alpha\Delta H_e}{2(1+\alpha)E_{e,0}}\right), \quad (13)$$

$$r^{\#}(\text{X}\ldots\text{H}) \approx r(\text{X–H}) + \frac{\alpha\beta\sqrt{E_{e,0}}}{b}\left(1 - \frac{\Delta H_e}{2(1+\alpha)E_{e,0}}\right). \quad (14)$$

These relationships show that linear expressions are valid for $|\Delta H_e| < 2(1 + \alpha)E_{e,0}$, while they lose their physical meaning for $|\Delta H_e| > 2(1 + \alpha)E_{e,0}$. The data calculated for the reactions of the triethylsilyl radical with hydrocarbons (RH) and silanes are presented in Tables 6 and 7. Those for the reactions of the $Ge^{\bullet}H_3$ and $Sn^{\bullet}H_3$ radicals with RH are given in Tables 8 and 9. These tables contain the enthalpies, activation energies, and rate constants calculated by formulas (1)–(5) for the reactions in question along with the $r^{\#}$(Y…H) and $r^{\#}$(X…H) values calculated using formulas (9) and (10).

For the reactions in which the $R_3Si^{\bullet}$, $R_3Ge^{\bullet}$, or $R_3Sn^{\bullet}$ radical is attacking, the $r^{\#}$(R…H) distance elongates with an increase in the enthalpy of reaction, whereas $r^{\#}$(H…Y) shortens (Y = Si, Ge, or Sn) (Fig. 3).

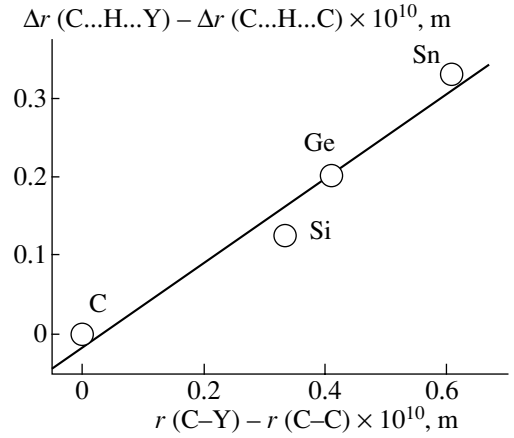

Fig. 4. Bond extension $\Delta r^{\#}$(C…H…Y) – $\Delta r^{\#}$(C…H…C) in the TS versus the bond length difference r(Y–C) – r(C–C) for the hydrogen atom abstraction reaction $Me_2C^{\bullet}H + R_3Y{-}H \longrightarrow Me_2CH_2 + R_3Y^{\bullet}$, where Y = C, Si, Ge, and Sn.

Table 6. Enthalpy, activation energy, rate constant, and TS geometry calculated by formulas (1)–(5), (9), and (10) for hydrogen atom abstraction from alkanes, alkenes, and alkylaromatic hydrocarbons by the $Et_3Si^{\bullet}$ radical

Compound R–H	D(R–H), kJ/mol	ΔH_e, kJ/mol	E, kJ/mol	k (350 K), l mol^{-1} s^{-1}	$r^{\#}$(C...H) × 10^{10}, m	$r^{\#}$(Si...H) × 10^{10}, m
			R^1–H			
$(Me_2CH)_2NMe_2C–H$	370.0	–23.7	26.9	2.0×10^5	1.342	1.888
$(Me_2CHNH)Me_2C–H$	375.0	–18.7	29.5	8.0×10^4	1.349	1.881
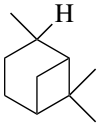	377.4	–16.3	30.7	5.2×10^4	1.352	1.878
$Me_2(NH_2)C–H$	379.5	–14.2	31.8	3.5×10^4	1.356	1.874
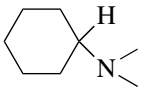	381.0	–12.7	32.6	2.7×10^4	1.358	1.872
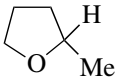	384.1	–9.6	34.3	1.5×10^4	1.362	1.868
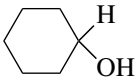	388.4	–5.3	36.7	6.7×10^3	1.369	1.861
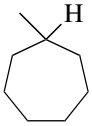	390.0	–3.7	37.6	4.9×10^3	1.371	1.859
BuO(CH–H)Pr	392.2	–1.5	38.8	6.5×10^3	1.374	1.856
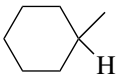	395.5	1.8	40.7	1.7×10^3	1.379	1.851
$Me_2(C–H)CHMe_2$	396.4	2.7	41.2	2.9×10^3	1.380	1.850
Pr(HO)CH–H	397.0	3.3	41.5	2.5×10^3	1.381	1.849
$Me_3C–H$	400.0	6.3	43.3	7.0×10^2	1.385	1.845
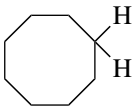	401.0	7.3	43.8	9.2×10^3	1.387	1.843
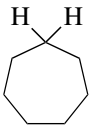	403.9	10.2	45.5	4.5×10^3	1.391	1.839
$(Me_2CH)_2MeC–H$	405.4	11.7	46.4	2.4×10^2	1.393	1.837
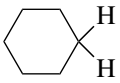	408.8	15.1	48.4	1.4×10^3	1.398	1.832
$Me_2CH–H$	412.0	18.3	50.4	1.2×10^2	1.402	1.828
BuEtCH–H	414.5	20.8	51.9	7.2×10^1	1.406	1.824
$Me_2(HO)CCH_2–H$	417.4	23.7	53.7	1.8×10^2	1.410	1.820
	418.5	24.8	54.3	1.2×10^2	1.412	1.818
$MeCH_2–H$	422.0	28.3	56.5	4.4×10	1.417	1.813
	429.0	35.3	61.0	9.6	1.426	1.804

Table 6. (Contd.)

Compound R–H	D(R–H), kJ/mol	ΔH_e, kJ/mol	E, kJ/mol	k (350 K), l mol^{-1} s^{-1}	$r^{\#}$(C...H) × 10^{10}, m	$r^{\#}$(Si...H) × 10^{10}, m
			R^2–H			
$(CH_2{=}CH)_2MeC{-}H$	307.2	–86.5	6.8	9.7×10^6	1.274	2.003
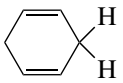	312.6	–81.1	8.9	1.9×10^7	1.282	1.995
$(CH_2{=}CH)_2CH{-}H$	318.0	–75.7	11.0	4.6×10^6	1.290	1.987
$CH_2{=}(CH)_2{=}CH(CH{-}H)Me$	321.1	–72.6	12.2	3.0×10^6	1.295	1.983
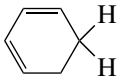	330.9	–62.8	16.4	1.5×10^6	1.309	1.968
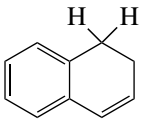	336.5	–57.2	18.8	3.1×10^5	1.317	1.960
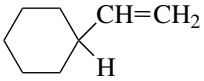	341.8	–51.9	21.2	6.9×10^4	1.325	1.953
Z-MeCH=CH(CH–H)Me	344.0	–49.7	22.2	9.7×10^4	1.328	1.949
$CH_2{=}CMe(CH{-}H)Me$	347.2	–46.5	23.7	5.8×10^4	1.332	1.945
$CH_2{=}CH(CH{-}H)Pr$	349.8	–43.9	24.9	3.8×10^4	1.336	1.941
$MeCH{=}C(CH_2{-}H)Me$	352.4	–41.3	26.2	7.5×10^4	1.340	1.937
E-$MeCH{=}CHCH_2{-}H$	356.8	–36.9	28.3	3.6×10^4	1.346	1.931
$CH_2{=}C(CH_2{-}H)Et$	367.7	–26.0	33.8	2.7×10^3	1.361	1.916
$CH_2{=}CHCH_2CH_2{-}H$	410.9	17.2	57.8	7.0×10^{-1}	1.420	1.857
$CH_2{=}C{-}HMe$	459.0	65.3	88.6	5.9×10^{-6}	1.482	1.795
			R^3–H			
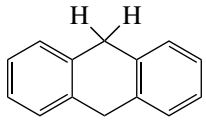	322.0	–71.7	8.0	2.5×10^7	1.279	1.970
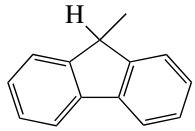	328.5	–65.2	10.6	2.6×10^6	1.289	1.960
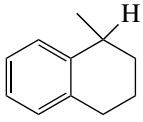	336.4	–57.3	14.0	8.2×10^5	1.301	1.948
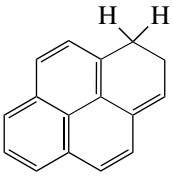	341.4	–52.3	16.2	7.7×10^5	1.308	1.940
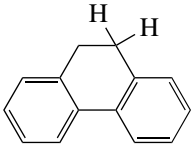	343.7	–50.0	17.2	1.1×10^6	1.312	1.937

Table 6. (Contd.)

Compound R–H	D(R–H), kJ/mol	ΔH_e, kJ/mol	E, kJ/mol	k (350 K), l mol^{-1} s^{-1}	$r^{\#}$(C...H) × 10^{10}, m	$r^{\#}$(Si...H) × 10^{10}, m
Ph_3C–H	346.0	–47.7	18.3	1.9×10^5	1.315	1.933
Ph_2MeC–H	348.8	–44.9	19.5	1.2×10^5	1.319	1.929
$PhMe_2C$–H	354.7	–39.0	22.3	4.7×10^4	1.328	1.920
Ph_2CH–H	356.8	–36.9	23.3	6.6×10^4	1.331	1.917
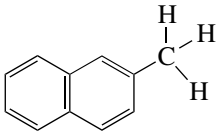	358.3	–35.4	24.1	7.7×10^4	1.333	1.915
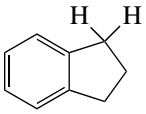	359.4	–34.3	24.6	8.5×10^4	1.335	1.914
PhMeCH–H	364.1	–29.6	26.9	1.9×10^4	1.342	1.907
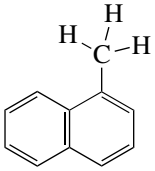	365.1	–28.6	27.4	2.4×10^4	1.343	1.905
PhPrCH–H	368.7	–25.0	29.3	8.6×10^3	1.349	1.900
$PhCH_2$–H	375.0	–18.7	32.5	4.2×10^3	1.358	1.891
(PhC)Me_2CH_2–H	412.6	18.9	53.8	2.8	1.411	1.838

For all of these reactions, there is a linear relationship of the type $r^{\#} = F + G\Delta H_e$ between $r^{\#}$(H…Y) and ΔH_e and between $r^{\#}$(X…H) and ΔH_e (Figs. 2, 3). The F and G data calculated using formulas (13) and (14) are given in Table 10. They enable one to calculate, using the ΔH_e value, the TS interatomic distances for the reactions obeying the inequality $|\Delta H_e| < 2(1 + \alpha)E_{e,0}$.

Atomic Radius

Equations (13) and (14) make it possible to estimate the elongation of the H–Y and C–H bonds for $\Delta H_e = 0$ and thus exclude the effect of the enthalpy of reaction on the TS geometry. Previously, we demonstrated that, the longer the H–Y bond in the YH molecule, the higher the activation energy of the thermally neutral abstraction reaction, $E_{e,0}$ [1]. The bond extensions in the TS for the thermally neutral reactions are listed in Table 11: $\Delta r^{\#}$(H…Y) = $r^{\#}$(H…Y) – r(H–Y), $\Delta r^{\#}$(R^1…H) = $r^{\#}$(R^1…H) – r(R^1–H), and $\Delta r^{\#}$(R^1…H…Y) = $r^{\#}$(R^1…H) + $r^{\#}$(H…Y) – r(H–Y) – r(R^1–H). The values of the bond length r(R^1–Y), which is the equilibrium distance between the C and Y atoms in the R^1–YR_3 molecule, are given for comparison. Here, r(H–Y) and r(R^1–H) are the equilibrium distances between the atoms H and Y and between C and H in the molecules. Their values are specified in the calculation procedure, and the r(R^1–Y) values are taken from a handbook [15].

Clearly, the H…Y and R^1…H distances in the TS of the thermally neutral abstraction reaction elongate with an increase in the C–Y bond length in the R^1–YR_3 molecule. The total extension of the H–Y and R^1–H bonds in the TS is linearly related to the C–Y bond length in the R^1–YR_3 molecule (Fig. 4). This relationship is analytically expressed as

$$\Delta r^{\#}(\text{C…H…Y}) = 0.53 \times 10^{-10}\ \text{m} + (0.49 \pm 0.08)(r(\text{C–Y}) - r(\text{C–C})). \quad (15)$$

The Y–H and R–H bond extensions also change in the same way as the radius of the Y atom. In the TS of a reaction of the type R$^{\bullet}$ + HY, the H atom is equidistant from the C and Y atoms only in a symmetric TS, where R = Y. As can be seen from the data in Table 12, the longer the H–Y bond, the greater the H–Y bond extension. The C–H bond extension in the TS also depends on the H–Y bond length. It increases with an increase in the H–Y bond length. These quantities are compared in Table 12.

Table 7. Enthalpy, activation energy, rate constant, and TS geometry calculated by formulas (1)–(5), (9), and (10) for hydrogen atom abstraction from silanes by the $Et_3Si^{\bullet}$ radical

Compound R_3Si–H	D(Si–H), kJ/mol	ΔH_e, kJ/mol	E, kJ/mol	k (350 K), l mol^{-1} s^{-1}	$r^{\#}$(Si...H) × 10^{10}, m	$r^{\#}$(Si...H) × 10^{10}, m
$(Me_3Si)_3Si$–H	351.0	–47.0	14.7	1.3×10^7	1.702	1.848
Ph_3Si–H	354.8	–43.2	16.1	7.9×10^6	1.708	1.842
Ph_2MeSi–H	359.2	–38.8	17.8	4.4×10^6	1.715	1.835
$(Me_3C)_3Si$–H	362.3	–35.7	19.1	2.9×10^6	1.719	1.831
$PhMe_2Si$–H	364.0	–34.0	19.7	2.3×10^6	1.722	1.828
$(MeS)_3Si$–H	366.0	–32.0	20.6	1.7×10^6	1.725	1.825
PhMeClSi–H	369.6	–28.4	22.1	1.0×10^6	1.731	1.819
$(Me_3C)_2MeSi$–H	372.8	–25.2	23.5	6.3×10^5	1.736	1.814
$(Me_3Si)Me_2Si$–H	378.0	–20.0	25.7	2.9×10^5	1.744	1.806
Cl_3Si–H	382.0	–16.0	27.5	1.5×10^5	1.750	1.800
H_3Si–H	384.1	–13.9	28.5	4.4×10^5	1.753	1.797
MeH_2Si–H	386.0	–12.0	29.4	2.5×10^5	1.756	1.794
Me_2HSi–H	391.7	–6.3	32.1	6.5×10^4	1.765	1.785
Et_3Si–H	398.0	0	35.2	1.1×10^4	1.775	1.775
F_3Si–H	419.0	21.0	46.3	2.5×10^2	1.808	1.742

The IPM data presented show that, the longer the radius of the Y atom (Y = C, Si, Ge, Sn), that is, the H–Y bond length, the greater the elongation of the interatomic distances H…Y and R…H. However, the R…H distance changes to a lesser extent as compared to H…Y. Therefore, the H…Y distance in the TS depends on the radius of the attacked (or attacking) Y atom: the longer the equilibrium distance r(H–Y) in the molecule, the longer the H…Y distance in the TS. This is also true for the reactions of silyl radicals with silanes, for which the total bond extension is $\Delta r^{\#}$(Si…H…Si) = 0.584 × 10^{-10} m, which is 0.054 × 10^{-10} m longer than that for the reactions $R^{1\bullet}$ + R^1H, for which $\Delta r^{\#}$(C…H…C) = 0.53 × 10^{-10} m [16].

Influence of β–π Bonds

This influence leads to opposite effects for the reaction product and TS. For instance, the resulting radical is stabilized when an unpaired reaction is conjugated with the π system. This is manifested as a decrease in the dissociation energy of the C–H bond in the allyl- and benzyl-containing compounds. By contrast, in the TS, the interaction between the electrons of the occupied three-center bonding orbital, which is delocalized over the C…H…Y reaction center, and π electrons with a similar orbital energy has a character of four-electron repulsion and results in the destabilization of the TS (Fig. 5).

Therefore, in radical abstraction involving the activated C–H bond, the activation energy of the thermally neutral reaction increases despite the decrease in the energy of the final state. Conversely, the effects of triplet repulsion in these systems somewhat stabilizes the TS, because the spin density on the C atom in the reaction center decreases. Using data characterizing the TS geometry in the reaction of the methyl radical with ethane and propylene [16], we found, in the B3LYP/6-311++G** approximation, that the energy of the CH_3 and C_2H_5 fragments in the triplet state is higher than the energy of the noninteracting radicals by 46.4 kJ/mol. At the same time, the energy of the CH_3 and $CH_2CH{=}CH_2$ fragments in the triplet state is higher than the energy of the noninteracting fragments by 36.6 kJ/mol. The corresponding relative energies of the fragments in the singlet state (with a distorted spin symmetry) are equal to 63.9 kJ/mol for the first case and 46.8 kJ/mol for the second.

The calculated E, $r^{\#}$(H…Si), and $r^{\#}$(C…H) data for the reactions of the triethylsilyl radical with α-C–H bonds of olefins (R^2H) and alkylaromatic hydrocarbons (R^3H) are presented in Table 6. Compare the inter-

Table 8. Enthalpy, activation energy, rate constant, and TS geometry calculated by formulas (1)–(5), (9), and (10) for hydrogen atom abstraction from organic compounds by the $Bu_3Ge^{\bullet}$ radical

Compound R–H	D(R–H), kJ/mol	ΔH_e, kJ/mol	E, kJ/mol	k (350 K), l mol^{-1} s^{-1}	$r^{\#}$(C...H) $\times 10^{10}$, m	$r^{\#}$(Ge...H) $\times 10^{10}$, m
$(Me_2CH)_2NMe_2C$–H	370.0	27.5	63.1	7.7×10^{-1}	1.454	1.916
$(Me_2CHNH)Me_2C$–H	375.0	32.5	66.2	2.6×10^{-1}	1.461	1.909
$PhCH_2$–H	375.0	32.5	66.2	7.9×10^{-1}	1.461	1.909
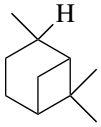	377.4	34.9	67.7	1.6×10^{-1}	1.464	1.906
$Me_2(NH_2)C$–H	379.5	37.0	69.1	9.8×10^{-2}	1.467	1.903
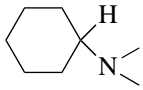	381.0	38.5	70.0	7.1×10^{-2}	1.469	1.901
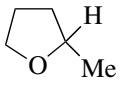	384.1	41.6	72.0	3.6×10^{-2}	1.474	1.896
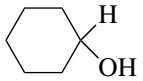	388.4	45.9	74.8	1.4×10^{-2}	1.480	1.890
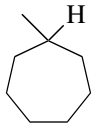	390.0	47.5	75.9	9.4×10^{-3}	1.482	1.888
BuO(CH–H)Pr	392.2	49.7	77.3	1.1×10^{-2}	1.485	1.885
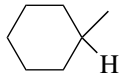	395.5	53.0	79.5	2.7×10^{-3}	1.490	1.880
$Me_2(C–H)CHMe_2$	396.4	53.9	80.1	4.4×10^{-3}	1.491	1.879
Pr(HO)CH–H	397.0	54.5	80.5	3.8×10^{-3}	1.492	1.878
Me_3C–H	400.0	57.5	82.6	9.6×10^{-4}	1.496	1.874
$(Me_2CH)_2MeC$–H	405.4	62.9	86.2	2.7×10^{-4}	1.503	1.867
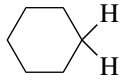	408.8	66.3	88.6	1.5×10^{-3}	1.508	1.862
Me_2CH–H	412.0	69.5	90.8	1.1×10^{-4}	1.512	1.858
BuEtCH–H	414.5	72.0	92.5	6.3×10^{-5}	1.516	1.854
$Me_2(HO)CCH_2$–H	417.4	74.9	94.5	1.4×10^{-4}	1.520	1.850
	418.5	76.0	95.3	9.5×10^{-5}	1.521	1.849
$MeCH_2$–H	422.0	79.5	97.8	3.1×10^{-5}	1.526	1.844
	429.0	86.5	102.8	5.5×10^{-6}	1.536	1.834

Table 9. Enthalpy, activation energy, rate constant, and TS geometry calculated by formulas (1)–(5), (9), and (10) for hydrogen atom abstraction from organic compounds by the $Bu_3Sn^{\bullet}$ radical

Compound R–H	D(R–H), kJ/mol	ΔH_e, kJ/mol	E, kJ/mol	k (350 K), l mol^{-1} s^{-1}	$r^{\#}$(C...H) × 10^{10}, m	$r^{\#}$(Sn...H) × 10^{10}, m
$(Me_2CH)_2NMe_2C$–H	370.0	65.7	89.1	1.3×10^{-4}	1.557	2.107
$(Me_2CHNH)Me_2C$–H	375.0	70.7	92.6	3.8×10^{-5}	1.565	2.099
$PhCH_2$–H	375.0	70.7	92.6	1.1×10^{-4}	1.565	2.099
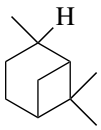	377.4	73.1	94.3	2.1×10^{-5}	1.569	2.095
$Me_2(NH_2)C$–H	379.5	75.2	95.8	1.3×10^{-5}	1.572	2.092
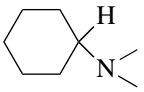	381.0	76.7	96.8	8.9×10^{-6}	1.574	2.090
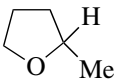	384.1	79.8	99.0	4.2×10^{-6}	1.579	2.085
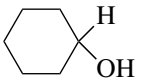	388.4	84.1	102.1	1.4×10^{-6}	1.585	2.079
BuO(CH–H)Pr	392.2	87.9	104.9	1.1×10^{-6}	1.591	2.073
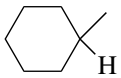	395.5	91.2	107.3	2.5×10^{-7}	1.596	2.068
$Me_2(C–H)CHMe_2$	396.4	92.1	107.9	3.9×10^{-7}	1.597	2.067
Pr(HO)CH–H	397.0	92.7	108.4	3.4×10^{-7}	1.598	2.066
Me_3C–H	400.0	95.7	110.6	7.9×10^{-8}	1.603	2.061
$(Me_2CH)_2MeC$–H	405.4	101.1	114.6	2.0×10^{-8}	1.611	2.053
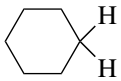	408.8	104.5	117.1	1.0×10^{-7}	1.616	2.048
Me_2CH–H	412.0	107.7	119.5	7.3×10^{-9}	1.621	2.043
BuEtCH–H	414.5	110.2	121.4	3.8×10^{-9}	1.624	2.040
$Me_2(HO)CCH_2$–H	417.4	113.1	123.6	8.0×10^{-9}	1.628	2.036
	418.5	114.2	124.5	5.3×10^{-9}	1.630	2.034
$MeCH_2$–H	422.0	117.7	127.1	1.6×10^{-9}	1.635	2.029
	429.0	124.7	132.5	2.5×10^{-10}	1.645	2.019

Table 10. Parameters F and G calculated by formulas (13) and (14) for the function $r^{\#} = F + G\Delta H_e$, where $r^{\#}$ is the interatomic distance (H...Y) or (X...H) in the TS

Reaction	$r^{\#}$(H...Y)		$r^{\#}$(X...H)	
	$F \times 10^{10}$, m	$G \times 10^{13}$, m mol kJ^{-1}	$F \times 10^{10}$, m	$G \times 10^{13}$, m mol kJ^{-1}
$Et_3Si^{\bullet} + R_3Si–H$	1.775	1.558	1.775	–1.558
$Me_2C^{\bullet}H + R_3Ge–H$	1.956	1.473	1.523	–1.473
$Me_2C^{\bullet}H + R_3Sn–H$	2.211	1.659	1.592	–1.659
$Et_3Si^{\bullet} + R–H$	1.376	–1.447	1.767	1.447
$Bu_3Ge^{\bullet} + R–H$	1.414	–1.473	1.847	1.473
$Bu_3Sn^{\bullet} + R–H$	1.452	–1.659	2.071	1.659

Table 11. Extensions of the H...Y and C...H bonds and their sums in the TS for the thermally neutral reactions of H atom abstraction by the alkyl radical ($R^{1\bullet}$)

Reaction	$\Delta r^{\#}(R^1...H...Y) \times 10^{10}$, m	$\Delta r^{\#}(H...Y) \times 10^{10}$, m	$\Delta r^{\#}(R^1...H) \times 10^{10}$, m	$r(R^1–Y) \times 10^{10}$, m
$R^{1\bullet} + R_3C–H$	0.530	0.265	0.265	1.536
$R^{1\bullet} + R_3Si–H$	0.655	0.370	0.285	1.870
$R^{1\bullet} + R_3Ge–H$	0.754	0.432	0.322	1.945
$R^{1\bullet} + R_3Sn–H$	0.860	0.500	0.360	2.144

Table 12. Extensions of the H...Y and R^1...H bonds in the TS for different H–Y bond lengths

Reaction	$r(H–Y) \times 10^{10}$, m	$(\Delta r^{\#}(H...Y) – 0.265) \times 10^{10}$, m	$(\Delta r^{\#}(R^1...H) – 0.265) \times 10^{10}$, m
$R^{1\bullet} + R^1–H$	1.092	0	0
$R^{1\bullet} + R_3Si–H$	1.483	0.105	0.020
$R^{1\bullet} + R_3Ge–H$	1.525	0.167	0.057
$R^{1\bullet} + R_3Sn–H$	1.711	0.235	0.095

Table 13. $r^{\#}$(C...H) distances as functions of ΔH_e for the reactions of the triethylsilyl radical with paraffins (R^1–H), olefins (R^2–H), and alkylaromatic hydrocarbons (R^3–H) and the correlation between $r^{\#}$(C...H) and the activation energy $E_{e,0}$ under thermally neutral conditions

Reaction	$r^{\#}(C...H) \times 10^{10}$, m	$E_{e,0}$, kJ/mol	$\Delta E_{e,0}$, kJ/mol	$\Delta r^{\#}(C...H) \times 10^{10}$, m at $\Delta H_e = 0$
$Et_3Si^{\bullet} + R^1–H$	$1.376 + 1.440 \times 10^{-3}\Delta H_e$	55.6	0	0
$Et_3Si^{\bullet} + R^3–H$	$1.385 + 1.460 \times 10^{-3}\Delta H_e$	58.7	3.1	0.009
$Et_3Si^{\bullet} + R^2–H$	$1.395 + 1.370 \times 10^{-3}\Delta H_e$	63.8	8.2	0.019

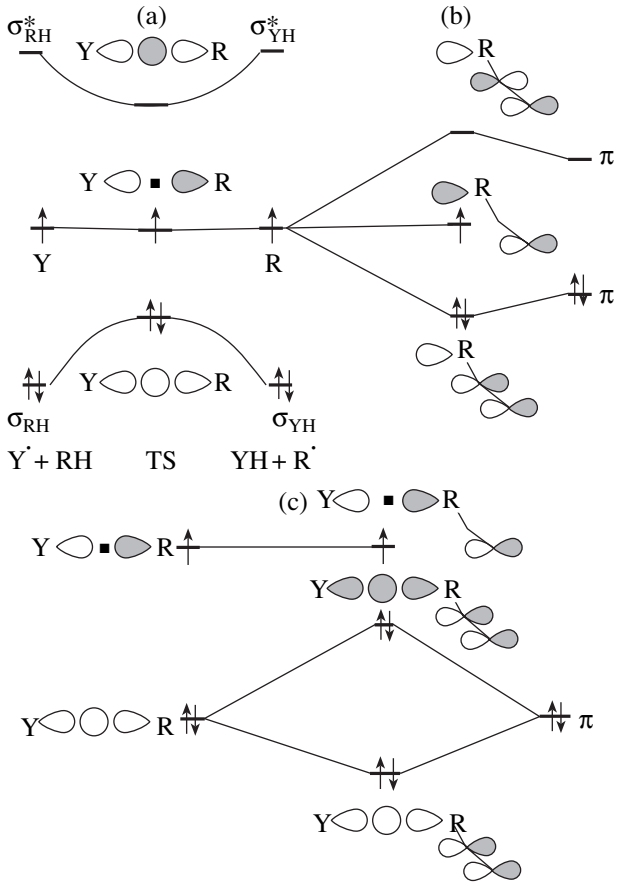

Fig. 5. Qualitative schemes of (a) the orbital interactions during radical abstraction and (b, c) the influence of a double bond in the β position relative to the radical center on the orbitals of the (b) product and (c) transition state.

atomic distances of the reaction classes $Et_3Si^{\bullet} + R^1H$, $Et_3Si^{\bullet} + R^2H$, and $Et_3Si^{\bullet} + R^3H$. In these three reaction classes, the dependence of $r^{\#}$(C…H) on ΔH_e is described by the equations given in Table 13.

Clearly, the $r^{\#}$(C…H) and $E_{e,0}$ parameters for ΔH_e = 0 change in the same way on passing from paraffins (R^1H) to olefins (R^2H) and alkylaromatic hydrocarbons (R^3H).

Note that the intermediate distances H…Y and C…H obtained by the quantum-chemical calculation (DFT) and formulas (13) and (14) (IPM) do not always coincide. These distances calculated using formulas (1), (5), (13), and (14) in the framework of the IPM are compared in Table 14.

These data show that the results of the two calculations for the first reaction, with $\Delta H_e = 0$, coincide. For the reactions of the methyl radicals with SiH_4, GeH_4, and SnH_4, the calculated Y…H and C…H distances calculated by these two methods differ by (0.15–0.27) × 10^{-10} m, although the total distances (C…Y) coincide.

Table 14. Comparison between the DFT and IPM values of the intermediate distances H...Y and C...H in the radical abstraction reactions

Reaction	$r^{\#}$(H...Y) × 10^{10}, m		$r^{\#}$(C...H) × 10^{10}, m	
	DFT	IPM	DFT	IPM
$Si^{\bullet}H_3 + SiH_4$	1.775	1.775	–	–
$C^{\bullet}H_3 + SiH_4$	1.614	1.766	1.616	1.461
$C^{\bullet}H_3 + GeH_4$	1.637	1.822	1.733	1.548
$C^{\bullet}H_3 + SnH_4$	1.780	2.056	1.884	1.608

CONCLUSIONS

The radii of the C, Si, Ge, and Sn atoms differ substantially. Therefore, the atomic radius of the reaction center is an essential factor in the TS of the radical abstraction reactions involving the Y…H bonds (Y = C, Si, Ge, Sn). The higher this radius, the greater the extension of both the C–H and Y–H bonds in the TS of the reactions $R^{\bullet}$ + HY. The total extension $\Delta r^{\#}$(R…H…Y) depends linearly on r(Y–R). Both the Y…H and R…H distances elongate with an increase in the R–Y bond length. The appearance of a π bond in the β position relative to the reaction center induces four-electron repulsion in the TS and increases the $\Delta r^{\#}$ value. The enthalpy of reaction also has an effect on the TS geometry: with an increase in ΔH_e in the $R^{\bullet}$ + HY reaction series, the Y…H distance elongates and the R…H distance shortens. The changes in the Y…H and R…H distances depend linearly on ΔH_e for $|\Delta H_e| < 2E_{e,0}(1 + \alpha)$.

ACKNOWLEDGMENTS

This work was supported by the Division of Chemistry and Materials Science of the Russian Academy of Sciences (Program no. 1: Theoretical and Experimental Investigation of the Nature of the Chemical Bond and Mechanisms of the Most Important Chemical Reactions and Processes).

REFERENCES

1. Drozdova, T.I. and Denisov, E.T., *Kinet. Katal.*, 2002, vol. 43, no. 1, p. 14.
2. Frisch, M.J., Trucks, G.W., Head-Gordon, M., Gill, P.M.W., Wong, M.W., Foresman, J.B., Johnson, B.G., Schlegel, H.B., Robb, M.A., Replogle, E.S., Gomperts, R., Andres, J.L., Raghavachari, K., Binkley, J.S., Gonzalez, C., Martin, R.L., Fox, D.J., Defrees, D.J., Baker, J., Stewart, J.J.P., and Pople, J.A., *Gaussian 98, Revision A.6*, Pittsburgh: Gaussian Inc., 1998.
3. Shestakov, A.F. and Denisov, E.T., *Izv. Akad. Nauk, Ser. Khim.*, 2003, no. 2, p. 306.
4. Arthur, N.L. and Bell, T.N., *Rev. Chem. Intermed.*, 1978, vol. 2, p. 37.

5. Roberts, B.P., *J. Chem. Soc., Perkin Trans.*, 1996, p. 2719.
6. Dakternieks, D., Henry, D.J., and Schiesser, C.H., *J. Chem. Soc., Perkin Trans. 2*, 1998, p. 591.
7. Dakternieks, D., Henry, D.J., and Schiesser, C.H., *J. Chem. Soc., Perkin Trans.*, 1997, p. 1665.
8. Song, L., Wu, W., Dong, K., Hiberty, P.C., and Shaik, S., *J. Phys. Chem. A*, 2002, vol. 106, p. 11361.
9. Pais, A.A.C.C., Arnaut, L.G., and Formosino, S.J., *J. Chem. Soc., Perkin Trans. 2*, 1998, p. 2577.
10. Wu, W., Cao, Z., Zhang, Q., and Shaik, S., *J. Phys. Chem. A*, 2002, vol. 106, p. 2721.
11. Denisov, E.T., *Usp. Khim.*, 1997, vol. 66, p. 953.
12. Denisov, E.T. and Denisova, T.G., *Handbook of Antioxidants*, Boca Raton, FL: CRC, 2000.
13. Denisov, E.T., *General Aspects of the Chemistry of Radicals*, Alfassi, Z.B., Ed., Chichester: Wiley, 1999, p. 79.
14. Denisov, E.T., Denisova, T.G., and Pokidova, T.S., *Handbook of Free Radical Initiators*, New York: Wiley, 2003.
15. *Handbook of Chemistry and Physics*, Lide, D.R., Ed., Boca Raton: CRC, 1993.
16. Denisov, E.T., Shestakov, A.F., Denisova, T.G., and Emel'yanova, N.S., *Izv. Akad. Nauk, Ser. Khim.*, 2004, no. 4, p. 693.